Appl Biochem Biotechnol (2010) 160:1188–1205
DOI 10.1007/s12010-009-8646-4

New Model for Polymerization of Oligomeric Alcohol Dehydrogenases into Nanoaggregates

Abolfazl Barzegar · Ali A. Moosavi-Movahedi · Anahita Kyani · Bahram Goliaei · Shahin Ahmadian · Nader Sheibani

Received: 22 December 2008 / Accepted: 12 April 2009 /
Published online: 15 May 2009

Abstract Polymerization and self-assembly of proteins into nanoaggregates of different sizes and morphologies (nanoensembles or nanofilaments) is a phenomenon that involved problems in various neurodegenerative diseases (medicine) and enzyme instability/inactivity (biotechnology). Thermal polymerization of horse liver alcohol dehydrogenase (dimeric) and yeast alcohol dehydrogenase (tetrameric), as biotechnological ADH representative enzymes, was evaluated for the development of a rational strategy to control aggregation. Constructed ADH nuclei, which grew to larger amorphous nanoaggregates, were prevented via high repulsion strain of the net charge values. Good correlation between the variation in scattering and λ^{-2} was related to the amorphousness of the nanoaggregated ADHs, shown by electron microscopic images. Scattering corrections revealed that ADH polymerization was related to the quaternary structural changes, including delocalization of subunits without unfolding, i.e. lacking the 3D conformational and/or secondary-ordered structural changes. The results demonstrated that electrostatic repulsion was not only responsible for disaggregation but also caused a delay in the onset of aggregation temperature, decreasing maximum values of aggregation and amounts of precipitation. Together, our results demonstrate and propose a new model of self-assembly for ADH

A. Barzegar
Research Institute for Fundamental Sciences (RIFS), University of Tabriz, Tabriz, Iran

A. Barzegar · A. A. Moosavi-Movahedi (✉) · A. Kyani · B. Goliaei · S. Ahmadian
Institute of Biochemistry and Biophysics, University of Tehran, Tehran, Iran
e-mail: moosavi@ibb.ut.ac.ir

A. A. Moosavi-Movahedi
Foundation for Advancement of Science and Technology in Iran (FAST-IR), Tehran, Iran

N. Sheibani
Department of Ophthalmology and Visual Sciences, School of Medicine and Public Health, University of Wisconsin, Madison, WI 53792, USA

N. Sheibani
Department of Pharmacology, School of Medicine and Public Health, University of Wisconsin, Madison, WI 53792, USA

enzymes based on the construction of nuclei, which grow to formless nanoaggregates with minimal changes in the tertiary and secondary conformations.

Keywords Self-assembly · Nanoensembles · Nucleation · Nanoaggregates · Net charge · Scattering correction · Polymerization · Electron microscopy

Introduction

Alcohol dehydrogenases (ADHs) are oxidoreductases, which are present in animal tissues, plants, and microorganisms. These enzymes have attracted major scientific interest because of their evolutionary perspectives, wide occurrence in nature, and their broad substrate specificity and stereo-selectivity [1]. ADHs are generally subdivided into three major groups [2]: (a) the short-chain zinc-independent ADHs [3], (b) medium-chain zinc-dependent ADHs (including horse liver [4] and yeast ADHs (isozymes I–III)) [5], and (c) the long-chain iron-activated ADHs [6]. ADHs play considerable roles in the processing and production of alcohols and acetic acid [7] and are uniquely suited for direct biomass fermentation to ethanol [8]. They also support the growth of methylotrophs, oxidize alcohols, and catalyze lignin degradation [7]. There is also a considerable interest in the use of ADHs in the chemical synthesis industry, particularly the pharmaceutical industry where the production of chiral compounds is an increasingly important step in the synthesis of chirally pure pharmaceutical agents [9, 10].

As industrial catalysts, enzymes must have robust activities that are stable under various chemical processes and thermal conditions. The potential biotechnological application of ADH enzymes, as chiral chemical catalysts, has long been recognized [11, 12]. The two medium-chain zinc-dependent ADHs, including yeast alcohol dehydrogenase (YADH) and horse liver alcohol dehydrogenase (HLADH), are among the first dehydrogenases studied as the representatives of ADH enzyme family. They have catalytic zinc ions, important cysteine residues, and homologous structures [13]. YADH is a tetramer of approximately 150 kDa, very similar in amino acid sequence to the mammalian dimeric ADH, the best studied of which is the dimeric HLADH. HLADH is composed of two identical subunits; each containing two zinc atoms. These enzymes are used for the synthesis of chiral compounds and widely studied for their well-known biotechnological significance [8, 14]. Unfortunately, both YADH and HLADH are unstable in aqueous solutions under thermal stress and can easily be aggregated [15–17], leading to phase separation and precipitation.

Stability, particularly the thermostability, is an important functional property of enzymes. ADHs are temperature labile in general. YADH is somewhat unstable even at 25°C [18]. Thermal treatment of proteins results in destabilization of the compact protein structure, which may lead to protein aggregation and precipitation. The aggregation of native soluble proteins, into insoluble inclusion bodies, is a serious concern in biotechnology and biomedical research. Both YADH and HLADH are thermally labile and easily aggregated. They have been used for many years as the model proteins to study the chaperone-like activity of many proteins such as α-crystallin, heat shock proteins [15–17], and β-caseins [19]. It is generally believed that the hydrophobic interactions result in protein aggregation. Therefore, many studies have focused on decreasing the hydrophobic interactions between proteins using different approaches such as: point mutations, residue modifications, solvent engineering by preferential hydration, and designing mini-chaperone peptides [20–23]. Recent studies, however, indicate that aggregation can often be reliably correlated with low net charges [20, 24]. Developing rational approaches to manage protein aggregation

requires a better understanding of the mechanisms that promote polymerization. Herein, evidence of the net charge and electrostatic repulsion effects on the suppression of YADH and HLADH aggregation and mechanistic view about their polymerization into aggregation are presented. Our results suggest that the disruption of native intersubunit contacts enforces the appearance of amorphous nanoaggregates by unfavorable interface into associated subunits without changing the protein's 3D conformation.

Materials and Methods

Crystallized and lyophilized HLADH, YADH, and NAD^+ were purchased from Sigma. Other chemicals were of analytical grade, obtained from Merck, and used without further purification. All solutions were prepared with double-distilled water and stored at 4°C before use.

Aggregation Assays

Time Dependency of Aggregation Assays

The ADH aggregation rates were determined by turbidity measurements, which cause an increase in optical density because of high scattering potency of larger aggregated macromolecules. The samples, including 0.1 mg/mL of HLADH or YADH, were placed in the thermostatic cell holder and the absorbance vs. wavelength was measured as a function of time. For the better analysis of aggregation process and its relationship with enzyme conformational changes, the samples were scanned within the range of 220–400 nm instead of a single wavelength. The OD values in each cuvette were recorded at 2-min intervals during the 60-min incubation at 55°C. All measurements were made while incubating ADHs in 50 mM sodium phosphate or pyrophosphate buffer (pH=7.0–9.5) at 55°C in a Carry-100 spectrophotometer, equipped with a ten-cell holder and a Peltier temperature control accessory.

Thermal Dependency of Aggregation Assays

Here, the stability of ADHs against the aggregation was evaluated under thermal stress, at different pHs (7.0–8.5). The amount of aggregation upon heating was determined by measuring the apparent absorption, due to scattering at 350 nm (OD 350) under the heat stress at 30–90°C. The experimental conditions were the same as those indicated for the above experiment.

Scattering Correction Analysis

Macromolecules such as proteins not only absorb but also scatter light and, therefore, appear to have an artificially high absorbance. Light scattering of the molecules, much smaller than the wavelength, is proportional to λ^{-4} [25], while the scattering of molecules, comparable in size or larger than the wavelength, is proportional to λ^{-2} [26].

The differences between the small and large molecules are due to homogeneous electric field strength over the molecules with the dimensions smaller than the wavelengths as compared to a different macromolecular excitation phase due to their various partitions. However, a scattering correction of protein samples can be made by measuring absorbance at a series of wavelengths far from the λ_{max}. As the macromolecular scattering varies with λ^{-2}, a plot of measured absorbance versus λ^{-2} (in the wavelength region far from the λ_{max})

was made. The degree of linearity of this plot may indicate the amounts of scattering by the macromolecules under study. The high degree of correlation coefficient of this fitted curve confirmed the existence of the scattering phenomenon in the macromolecule-containing solution. Extrapolation of the linear equation of $OD = a\lambda^{-2} + b$, derived from fitting the absorbance data (OD values) of the wavelength region far away from λ_{max}, to the wavelength region of λ_{max} gives the absorbance due to scattering. Coefficients "a" and "b" show the slope and intercept of linear equation and are used for the calculation of scattering amounts for the wavelength region of λ_{max}. The corrected absorbance values are calculated by subtracting the values of the absorbance spectrum from the values of scattering plots.

Analysis of Secondary Ordered Conformation

Secondary structures of ADHs (YADH and HLADH) were analyzed by circular dichroism (CD) AVIV spectropolarimeter, model 215. Far-UV CD studies were carried out with a 0.1-cm quartz cell, in the wavelength range of 190–260 nm at 25°C and at a pH range of 7.0–9.5. The enzyme concentration was 0.1 mg/mL in 50 mM phosphate or pyrophosphate buffer. For detailed analysis of the structural changes in protein, the CDNN software was used to determine the percentage of different types of secondary conformation in each sample.

EM Analysis of Aggregate Formation

Electron microscopy (EM) was used to evaluate the formation of larger-sized fibrils or the construction of amorphous nanoaggregates under heat stress. The samples of HLADH and YADH were incubated for 60 min at pH 7, the pH at which the ADHs readily begin to aggregate under thermal stress of 55°C. Following incubation, 3 μL of each ADH solution was applied to 400-mesh copper grids, coated with Formvar/carbon film for 30 s. Excess solution, on the other side of grids, was absorbed using a filter paper. The grids were stained with a drop of 1% aqueous filtered uranyl acetate for 20 s. The excess staining solution was absorbed using a filter paper and samples were air dried for 2 h. The grids were then examined under an electron microscope (HHU-12A Hitachi) at 75 kV.

Enzyme Activity Assays at Different pHs

The optimum pH of ADHs activity was determined by assaying the enzyme activity at 25°C and different pHs. The enzyme reactions were carried out in 50 mM phosphate/pyrophosphate buffer (pH=7.0–9.5) at 25°C, as described by our recent study [27]. Briefly, ethanol oxidation by ADH was carried out by using NAD^+ as a coenzyme, which is continuously reduced to NADH. NADH absorption, at 340 nm vs. time, is linearly related to ADH activity. In all cases, the activities were measured at least thrice. The specific activity (SA) values were normalized and reported, based on the %SA, for comparing the activity of HLADH and YADH at different pHs.

Results

ADH Turbidity Assays

Mesophilic ADH enzymes are more sensitive to high temperature and are readily aggregated. Figure 1 shows the absorbance values of samples at the pH of 7.0, 7.5, and

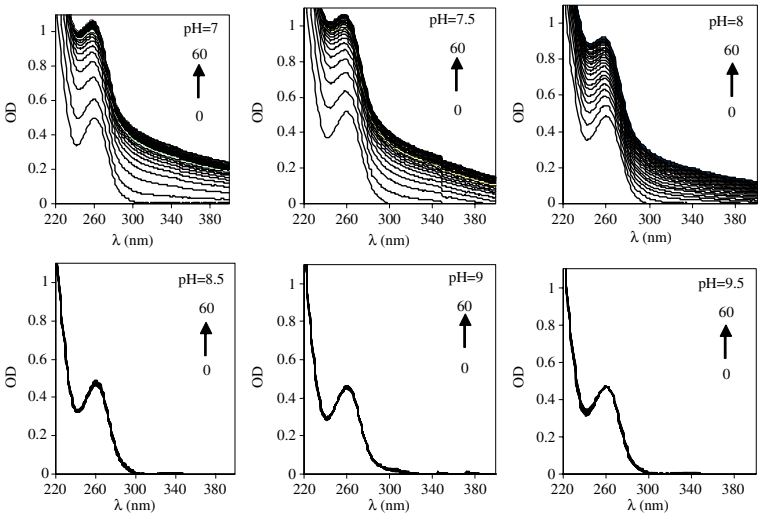

Fig. 1 Absorption spectra of HLADH at different pHs. The sequential increase in each spectrum was recorded at 2-min intervals during the incubation of HLADH enzyme at 55°C for 60 min

8.0, which increased for all ranges of the wavelengths (220−400 nm) studied throughout the incubation analysis at 55°C. It also shows that thermal stress causes the native soluble form of HLADH to be changed to a nonsoluble type of macromolecule during incubation, resulting in scattering. Scattering in macromolecule solutions is related to larger aggregated conformations. Hence, Fig. 1 indicates that increasing pH diminishes aggregation up to pH 8.0 and suppresses the aggregation at pH≥8.5 under thermal effects. Similar results were observed with the mesophilic YADH enzyme (Fig. 2).

Scattering Corrections and 3D Conformational Analysis

The use of scattering corrections gives useful information regarding the aggregation phenomenon as well as the 3D structural changes in macromolecular solution [28]. Scattering causes artificially high absorbance in a series of wavelengths even at λ_{max}. The λ_{max} is related to the absorbance of aromatic residues, which are usually employed for folding/unfolding studies and are related to 3D conformational changes. Therefore, scattering correction was made by measuring the absorbance at a series of wavelengths far from λ_{max} (300–400 nm). Absorbance changes at the wavelengths ≥300 nm were purely related to the scattering, derived from aggregation. Figures 3 and 4 (left panels) show a good linear relationship between the absorbance of both mesophilic ADHs vs. λ^{-2} (the wavelengths at the range of 300–400 nm) at a pH<8.5. A high linear correlation of OD values with λ^{-2} indicates comparable sizes for polydispersed molecules with the wavelength of 200–400 nm due to the aggregation phenomenon for both HLADH and YADH. Figures 3 and 4 (left panels) also show that there are not high values of R^2 for enzyme solutions at the zero time of incubation. This indicates the absence of scattering and so the lack of aggregation at the start of the experiment. The same type of plots, at pH>8.5 for both enzymes (plots are not shown for brevity), revealed a curvature treatment for the absorbance vs λ^{-2}, which indicates the nonlinearity of scattering results. If the size of sample solute is much smaller than the studied wavelengths, it is not possible to obtain a linear correlation with λ^{-2} [25, 26]. The nonlinearity of absorbance vs. λ^{-2} for the samples

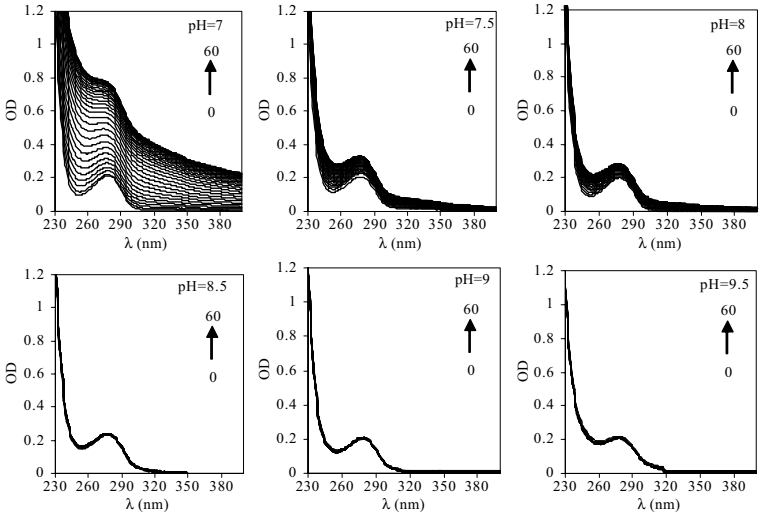

Fig. 2 Absorption spectra of YADH at different pHs. The experimental conditions were the same as in Fig. 1

free from aggregation, at pH>8.5, has indicated that the sizes of soluble ADH solutes are much smaller and noncomparable with the wavelength. However, a greater linear correlation between the absorbance and λ^{-2} confirms the polymerization of ADH molecules, leading to the construction of nanoaggregates, which are comparable with the size of related wavelength.

Scattering correction plots vs. λ, in Figs. 3 and 4 (right panels), were derived from the extrapolation of linear parts ($R^2 \geq 0.90$) with mentioned OD values vs. λ^{-2} for both ADH enzymes at a series of wavelengths. The absorbance spectra of the enzyme solutions, incubated for 60 min with and without scattering corrections, are also shown in Figs. 3 and 4 (right panels). They show that any absorbance variation in λ_{max} was compensated by subtracting the artificial absorbance values, based on the scattering. Superimposing the sample spectra, by scattering corrections, have indicated that heat stress for a long time (60 min at 55°C) had no effects on the 3D conformational changes of both ADHs. Thus, both ADHs readily aggregate under the heat stress without any significant 3D structural changes.

Charge Dependency of ADHs Physical Instability

Our results have indicated that pH≥8.5 suppresses the aggregation and/or any other conformational changes in both ADHs during the incubation times under thermal stress. It was exhibited that YADH aggregation is more dependent on the pH than HLADH. To better analyze this fact, the aggregation percentage was plotted for both ADHs vs. pH (Fig. 5). A rapid decrease in the aggregation quantity (85%) with increasing the pH from 7 to 7.5 was observed for YADH. In contrast, only 10% of initial aggregation value decreased for HLADH under similar conditions. An interesting observation of the experiment showed that at the pH≥8.5, the aggregation was completely suppressed for both YADH and HLADH. The isoelectric points (pI) of YADH [29] and HLADH [30] are 5.4 and 6.8, respectively. The pI is related to pH when the net charge of protein is zero. Higher pI is related to higher amounts of basic residues in the primary structure of proteins. Different residues that make up the primary structure of HLADH and YADH are listed in Table 1. As

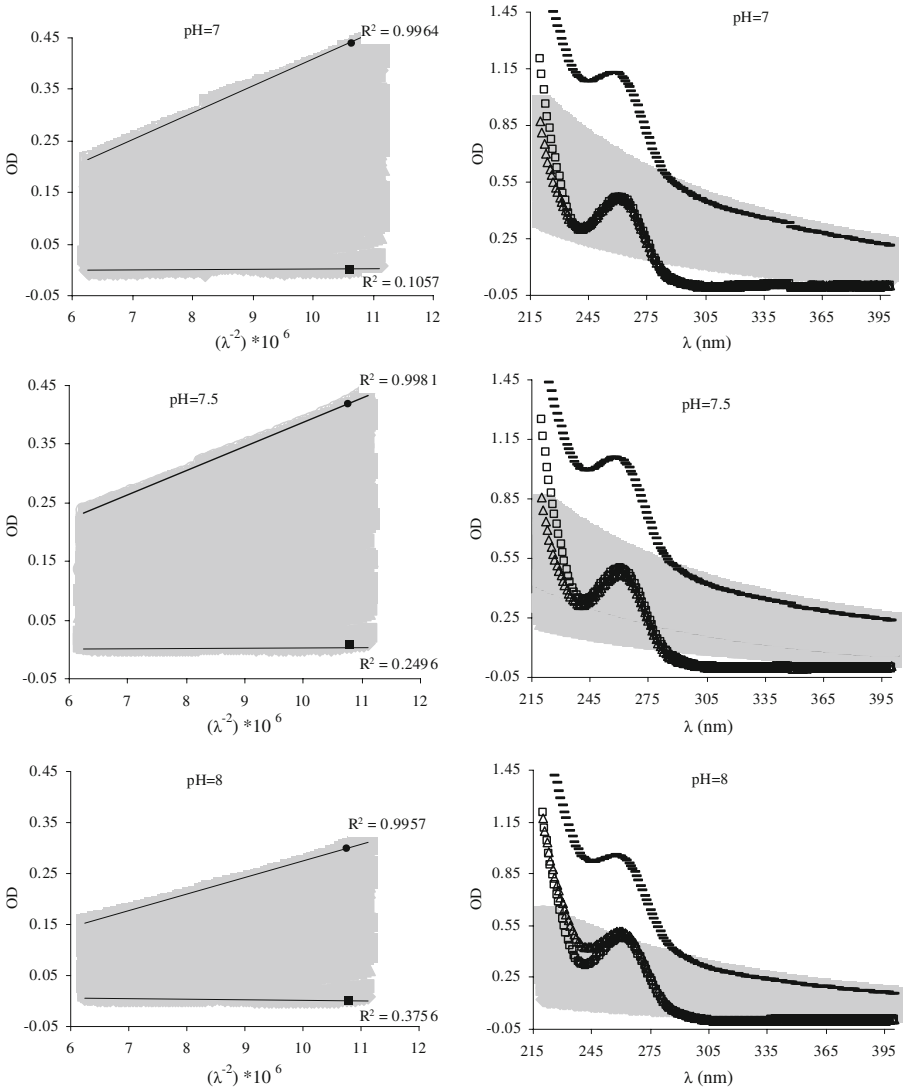

Fig. 3 Correlation of HLADH absorbance with λ^{-2} at different pHs (*left panels*) and scattering correction (*right panels*) for the entire series of wavelength region. The *gray shadows* indicate the range of scattering correlation with λ^{-2} (*left panels*) and λ (*right panels*) from zero to the last incubation time. None and good linear scattering correlation with λ^{-2} at zero time (*filled squares*) and the last incubation time of 60 min (*filled circles*), respectively. The spectra in *right panels*, at zero incubation time (*empty squares*), at last time of incubation before scattering correction (*dashes*) and after the scattering corrections (*empty triangles*) are depicted

expected, the basic residues were 1% more in HLADH than in YADH, whereas the acidic residues were almost the same. Hence, a 1% increase in basic residues is sufficient to increase the pI from 5.4 (YADH) to 6.8 (HLADH) and is responsible for slower aggregation slope in HLADH at pH 7.0–8.5. In addition, Table 1 signifies the same percentage of hydrophobic residues in the primary structure of both HLADH and YADH. Thus, a sharp decrease in the aggregation of YADH should be related to the differences in charge effects and not to the differences of hydrophobic interactions. pH changes is related to the changes

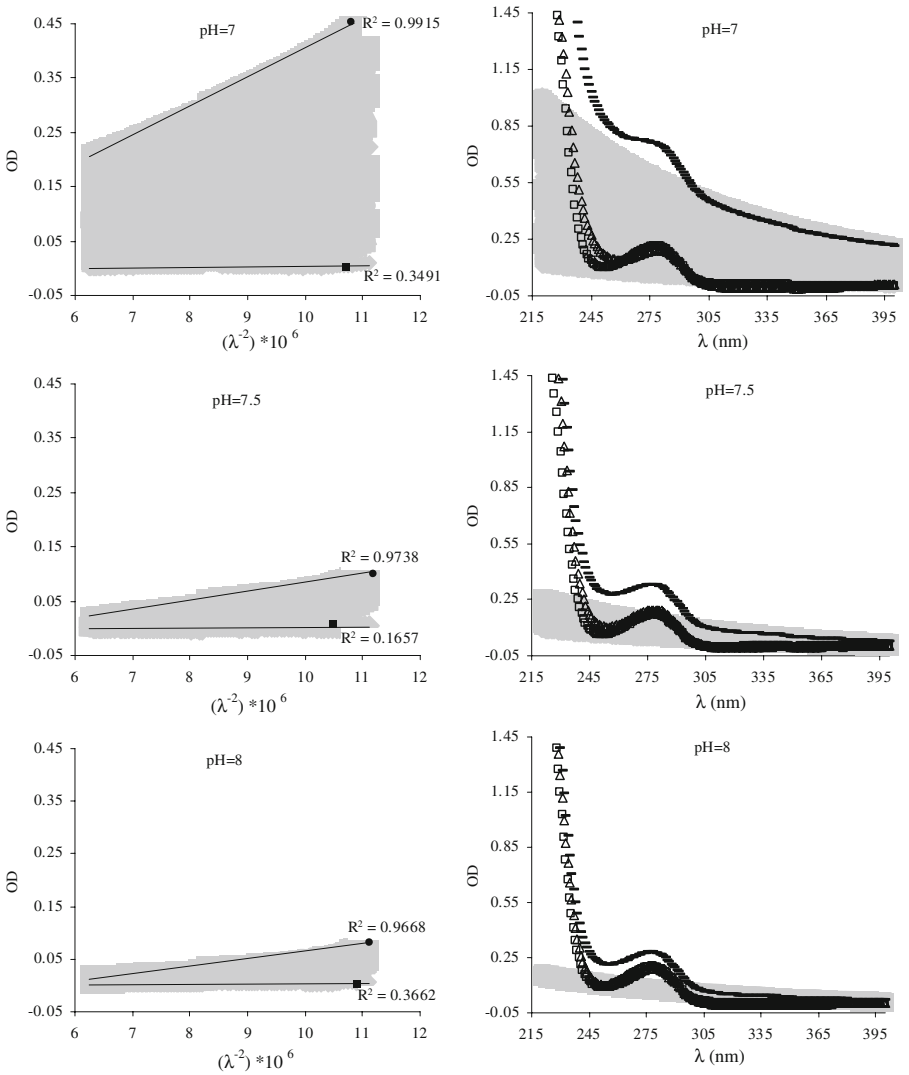

Fig. 4 Correlation of YADH absorbance with λ^{-2} at different pHs (*left panels*) and scattering corrections (*right panels*) for the entire series of wavelength region. The symbols and conditions of experiment were the same as for the Fig. 3

in net charge values of the enzymes. The net charge quantity of HLADH and YADH was calculated using PROPKa [31] and listed in Table 2. The net charge values indicated that the negative charge of YADH is greater than that of HLADH at the identical pH. Thus, because of less basic residues in YADH, which results in a lower pI value with higher negative charge, there exists a higher pH dependency for aggregation.

Thermal Scanning of ADHs and Charge Effects

Figure 6 shows turbidity measurements vs. thermal scanning (25–95°C), confirming the time-dependent net charge effects on the aggregation of both HLADH and YADH. Thus,

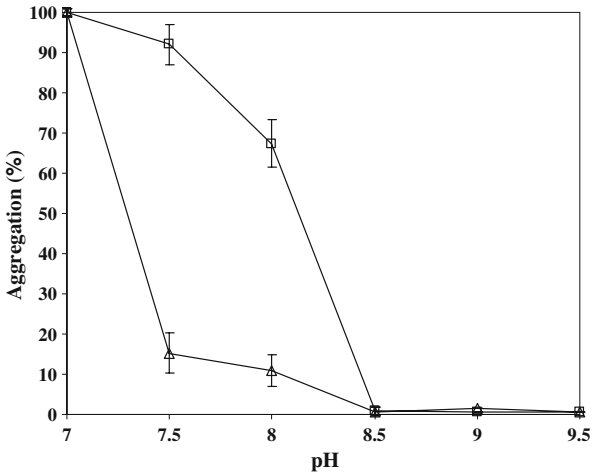

Fig. 5 The percentage of aggregation for YADH (*empty triangles*) and HLADH (*empty squares*) vs. pH after 60 min of incubation at 55°C. The values are acquired via normalization of aggregation at each pH by the relation $\frac{A_{pH7}}{A_{pHx}} \times 100$. A_{pH7} and A_{pHx} is related to the average value of turbidity, based on OD_{360nm} during 10 min from the end times of incubation (50–60 min) at pH 7 and other pHs, respectively

the increase in pH from 7.0 to 8.5 caused not only a delay in the aggregation temperature at least by 10° but also decreased maximum aggregation amount at the saturation phase. Another important observation was related to the precipitation of both HLADH and YADH, especially at pH=7.0. Precipitation caused phase separation of macromolecules, leading to decreased OD values at the temperatures above 75°C, representing the final state in aggregation process. Thus, these results emphasize the important role of net charge not only in decreasing and delaying the aggregation but also actively preventing the precipitation of both ADHs as well.

The Relationship Between the Aggregation and Secondary Structure of ADHs

To elucidate whether the aggregation of the two proteins can be attributed to the remarkable differences in nonnative β sheets, which were previously shown to be important determinants of the aggregation [32], we used Far-UV CD analysis, which is proven to be a powerful method to define secondary structure of macromolecules in solution. Far-UV CD results have shown no remarkable spectral differences for aggregated ADHs during the 30-min incubation at 55°C (Fig. 7). These findings confirmed the scattering corrected UV results in "Scattering Corrections and 3D Conformational Analysis", demonstrating little or no secondary and 3D structural changes in both ADHs during the aggregation under heat stress.

Table 1 The number of different group of amino acid residues in the primary structure of HLADH and YADH monomers.

ADHs	Basic a.a.	Acidic a.a.	Polar a.a.	Non Polar a.a.
HLADH	49 (13.1%)	38 (10.2%)	70 (18.7%)	217 (58.0%)
YADH	42 (12.1%)	36 (10.4%)	69 (19.9%)	200 (57.6%)

The numbers in parentheses indicate the related percentage of each group of amino acids. The Pdb structures of 1A71 and 2HCY were used by Swis-PdbViewer 3.7 to analyze HLADH and YADH, respectively

Table 2 Predictions of HLADH and YADH enzymes net charge as a function of pH using PROPKA [31].

Different pHs[a]	HLADH	YADH
pH=5	+9.67	+1.93
pH=6	+2.62	−5.07
pH=7	+1.06	−8.30
pH=8	−3.55	−10.12
pH=9	−7.66	−12.52
pH=10	−19.05	−21.40
pH=11	−36.94	−36.38
pH=12	−46.63	−46.55

The Pdb structures of 1A71 and 2HCY were used to calculate the HLADH and YADH geometry, respectively

[a] The pI values for HLADH and YADH were predicted to be 6.65 and 5.19, respectively. It is noteworthy that the predicted pI values are in agreement with the experimental values 6.8 [30] and 5.4 [29].

For analyzing the possibility of secondary structural changes in ADHs under increasing negative net charge, the percentage of different types of secondary structure was studied and evaluated by CDNN software (Tables 3, 4). CDNN (http://bioinformatik.biochemtech.uni-halle.de/cdnn/) was used to compute the percentage of different types of secondary structures in details. These results indicated that in aggregated ADH molecules, not only is there no induction of nonnative β sheet but also the transition of other types of secondary structures including α-helices, turns, and coils were almost invariant. Almost, all types of secondary structures such as helices, sheets, turns, and coils were unvaried under the experimental conditions (pH=7.0–9.5). However, the propensity to form nonnative β-sheet type of secondary structure (favorite structure in amyloid-fibril aggregates), even under favorable low net charge conditions of aggregation, was absent for both ADHs.

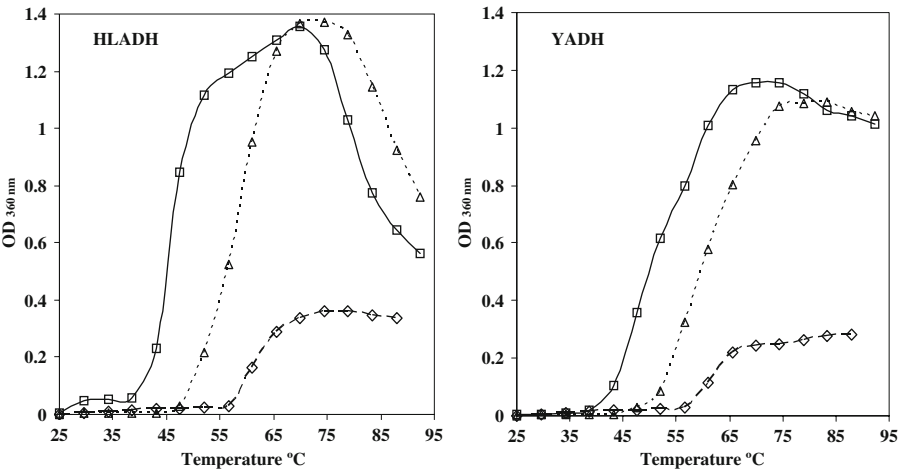

Fig. 6 Optical density (A_{360} nm) vs. scanning temperature of HLADH and YADH at different pHs (pH=7 (*empty squares*), pH=7.5 (*empty triangles*), and pH=8.5 (*empty diamonds*)

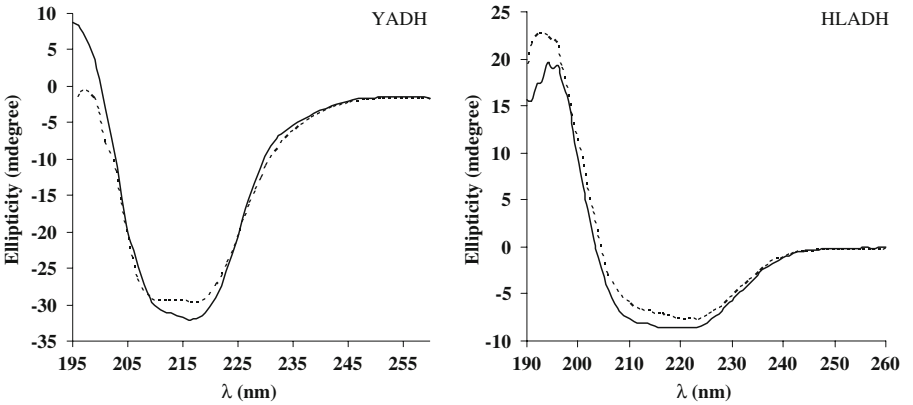

Fig. 7 Circular dichroism spectra of HLADH and YADH at 55°C, pH=7. *Filled lines* and *dashed lines* are related to zero time and 30 min of incubation at 55°C, respectively

Assessments of the Configuration of Nanoaggregates by EM

To determine whether amyloid-like filaments and/or amorphous nanoaggregates were formed or not, EM was used to examine the incubated ADHs under most favorable aggregation conditions at pH 7.0, as described in the "Materials and Methods" section. EM is a powerful method to analyze the configuration of recently formed aggregates [33]. Herein, EM was used to evaluate possibly fibril formation or construction of amorphous nanoaggregates of ADHs. Figure 8 illustrates no fibril formation or the appearance of any other known pattern conformers for aggregated ADHs. Construction of amorphous aggregates, free from fibril formation, was consistent with the CD results. Assessment of the secondary structure of aggregated ADHs, in Fig. 7, showed the lack of induction for any nonnative β sheets (fibril structures). EM images also indicate that the aggregation phenomenon results in the formation of different nanoparticles with broad sizes, possibly 10–1,000 nm. Thus, the configurations of aggregated enzymes are formless at nanoscale with different particles as a high polydispersion.

Charge Effects on Physical Stability and Enzyme Activity

Our findings are notable because net charges have two different effects: anti-aggregation and unfolding effects [34]. The favorable charge–charge interactions are important in determining the unfolded state ensemble [24]. Natively unfolded proteins have a total net charge that is generally higher in addition to having a lower content of hydrophobic

Table 3 The percentage of the secondary structure of HLADH at different pH obtained by cdnn program version 2 using CD Spectra.

Secondary St.	pH=7.0	pH=7.5	pH=8.0	pH=8.5	pH=9.0	pH=9.5
%Helix	17.1762	16.9714	17.079	16.5632	17.0567	16.4479
%Antiparallel	29.1231	30.4054	30.1277	32.7386	30.7021	33.1274
%Parallel	8.8898	8.5056	8.5395	7.9131	8.3697	7.9151
%Beta-turn	12.5503	12.5994	12.6496	12.6455	12.733	12.5869
%Random coil	32.2607	31.5183	31.6042	30.1396	31.1384	29.9228

Table 4 The percentage of the secondary structure of YADH at different pH obtained by CDNN program version 2 using CD spectra.

Secondary St.	pH=7.0	pH=7.5	pH=8.0	pH8.5	pH=9.0	pH=9.5
%Helix	15.6142	15.5009	16.1938	14.818	15.1228	15.35807
%Antiparallel	13.4083	13.4715	13.2693	13.7901	13.7441	13.54616
%Parallel	13.019	13.0829	12.8328	13.2334	13.1409	13.11475
%Beta-turn	17.6471	17.6166	17.6779	17.6874	17.751	17.68766
%Random coil	40.2249	40.3282	39.9825	40.3854	40.2413	40.29336

residues than those of proteins that fold into globular structures. To confirm that the extreme net charges under alkaline pH had negligible effect on the native conformation of enzymes, the activity of ADHs was assayed within the same environment. The results of the activity assays, for HLADH and YADH at various pHs, are shown in Fig. 9. These results indicate that the alkaline pH is most suitable for increased activity of ADH enzymes. The 3D structure of proteins determines their function. Thus, both YADH and HLADH were more active at pH 8–9. Thus, the optimum pH of the catalytic activity for both YADH and HLADH was 8.5.

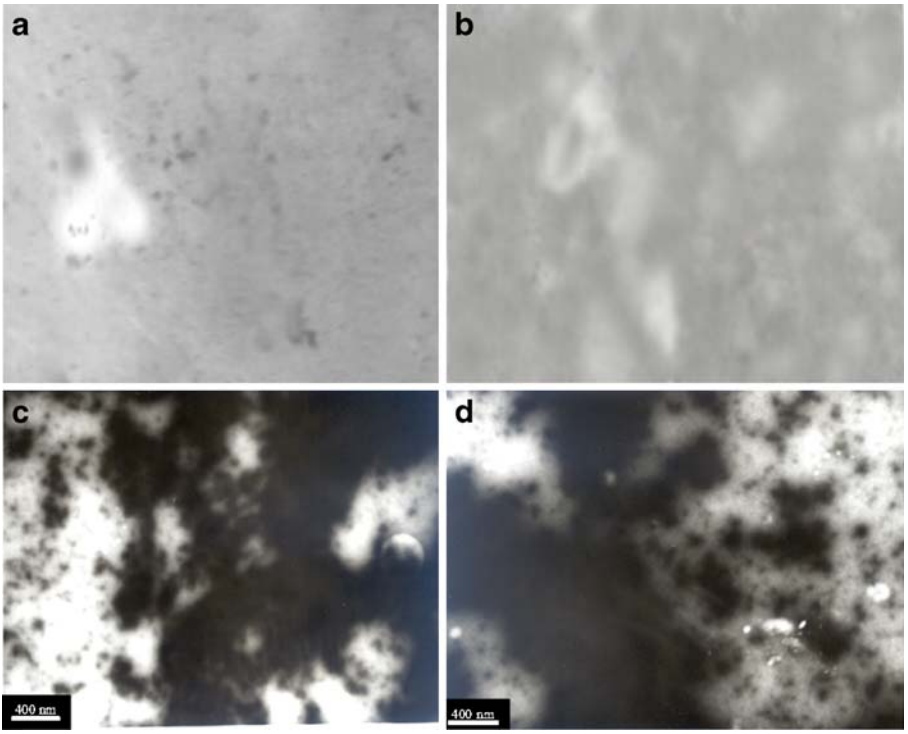

Fig. 8 EM analysis of amorphous aggregate formation in HLADH (**A**, **C**) and YADH (**B**, **D**) at different polydispersed nanoscale sizes. **A** and **B** are related to controls while **C** and **D** are related to incubated enzymes (0.1 mg/ml) at 55°C for 60 min

Discussion

Unlike crystallization and self-assembly processes, aggregation involves the association of thermo-labile conformation intermediates rather than the stable native protein. Controlling aggregation requires a clear understanding of the important factors that cause polymerization. Important factor, in decreasing turbidity and suppressing the aggregation for both ADHs, were based on the pH that is related to the net charge effects. Turbidity-caused augmentation of absorbance values for both HLADH and YADH at all wavelengths and pH 7.0, 7.5, and 8.0 during the incubation period. However, 3D structural changes in the absence of scattering generally caused an increase in absorbance only at λ_{max}. Appearance of larger aggregated molecules caused artificially increased absorbance and interfered with true absorbance values at λ_{max}. Therefore, we performed scattering correction by following λ^{-2} with a reliable correlation. Following the true absorbance (corrected scattering) at λ_{max} for both ADHs indicated no 3D conformational changes in the enzymes during aggregation. Evaluation of secondary ordered conformation by far-UV CD was related to the lack of any helix or sheet to coil transitions during the long incubation period under heat stress. Thus, these results strongly confirm the interesting phenomenon that ADHs aggregation occurs with minimal secondary and/or tertiary structural changes.

Protein aggregation is considered as an irreversible reaction, proceeding with the participation of n molecules of the nonnative conformations. First, aggregation is preceded by the protein's unfolding stage and secondly, the association of a number of unfolded states conformers:

$$N \rightarrow U \rightarrow (U+U)n \rightarrow A$$

N is the native state of the protein molecule and *U* is the unfolded state, which is prone to aggregation (*A*). Interaction of denatured protein molecules result in aggregation. The aggregation of monomeric proteins is a simple process and follows the indicated mechanisms [35]. It involves interactions of several protein molecules in the unfolded state, transforming into a larger aggregate. However, aggregation of oligomeric proteins,

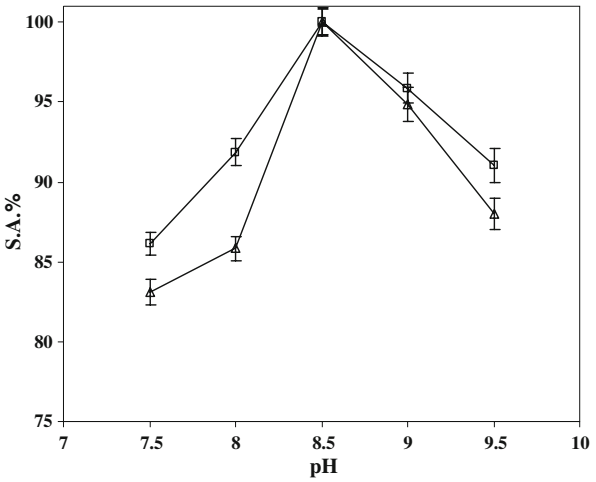

Fig. 9 The percentage of specific activity for HLADH (*empty squares*) and YADH (*empty triangles*) vs. pH. Activity was assayed in 50 mM phosphate buffer at pH 7.0–8.0, in 50 mM pyrophosphate buffer (pH=8.5–9.5). Each point represents the average quantity of at least three determinations

with different subunits, may occur via different mechanisms. Dissociation of subunits, under harsh conditions, such as thermal stress, is the first phenomenon that appears in oligomeric enzymes [36, 37]. Different subunits in oligomeric enzymes are linked to each other by special sites namely "conformational lock" [37]. Based on Poltorak theory [37–39], the thermal stress causes sequential disruption of conformational locks leading to subunit dissociation:

$$\mathrm{MM}n \rightarrow \mathrm{MM}n-1 \rightarrow \mathrm{MM}n-2 \rightarrow \mathrm{MM}n-3 \rightarrow \mathrm{M}+\mathrm{M}$$

The model includes three sequential stages for the formation of monomers in dimeric MM macromolecule by loosing three conformational locks (n=3). Monomerized subunits tend to achieve 3D conformational changes with unfolding and then association leads to aggregation by heat stress as it occurs in monomeric proteins.

$$\mathrm{MM}n \rightarrow n\mathrm{M}$$
$$n\mathrm{M} \rightarrow nU \rightarrow (U+U)n \rightarrow A$$

A possible mechanism, based on this theory, was proposed for ADHs aggregation in Scheme 1 by sequential **1**, **2**, and **3** reactions. In reaction **1**, the native dimeric HLADH (or tetrameric YADH) dissociate into monomers by breaking weak interactions in the quaternary structures at the conformational locks under thermal stress. Based on reaction **2**, the monomeric subunits loose native 3D conformation and denature. Finally, the unstable unfolded monomers tend to associate and lead to the aggregation in reaction **3**. However, our findings indicated that under aggregation process of ADHs, not only the 3D conformation of the enzymes is invariant but also their secondary structures do not change. Thus, the aggregation of oligomeric ADHs is different from the indicated usual mechanism in the reactions **1**, **2**, and **3**. Therefore, we proposed an alternative mechanism for the polymerization pathway of ADHs in reactions **1′** and **2′**. These processes indicate broken native locks in quaternary structures and the subunit dislocation by new unfavorable locks, built as an aggregation-prone state intermediate (*I*) without unfolding. Recently, we have shown that the appearance of *I* conformers during aggregation by chemometric PCA analysis, which had high affinity to bind chaperon like β-casein proteins (βCN) construct *I*-βCN. The *I*-βCNs complex suppressed the formation of final aggregated state of HLADH molecule [40]. The quaternary structural changes are the only possible conformational changes during aggregation phenomenon that leads to aggregation and are proposed as "*I*" conformers.

Hence, aggregation-prone state intermediate *I* should be related to the changes only in quaternary structure of enzymes, based on delocalization of subunits, without any changes in secondary/3D conformations of ADHs during aggregation. The *I* molecules can justify our previously reported nucleation-growth mechanism [27]. Three models, by kinetic mechanism of aggregation, include the sequential particle–cluster aggregation, multimeric cluster–cluster aggregation, and nucleation-dependent aggregation [41, 42]. Nucleation-growth pathway is characterized by slowly forming nucleus, followed by the rapid aggregate growth. This mechanism generates a sigmoidal-shaped curve in light scattering. Thus, the appearance of "*I*" molecules leads to the construction of nuclei, which is the first stage in aggregation phenomenon and tends to form larger amorphous aggregates. Therefore, the nucleation-growth pathway of delocalized lock subunits, in oligomeric ADHs, can illustrate the appearance of amorphousness aggregated nano-particles with high polydispersion.

Increasing the net charge suppresses aggregation by preventing the construction of *I* molecules, which are inclined to aggregation and associating the nuclei. The possible model

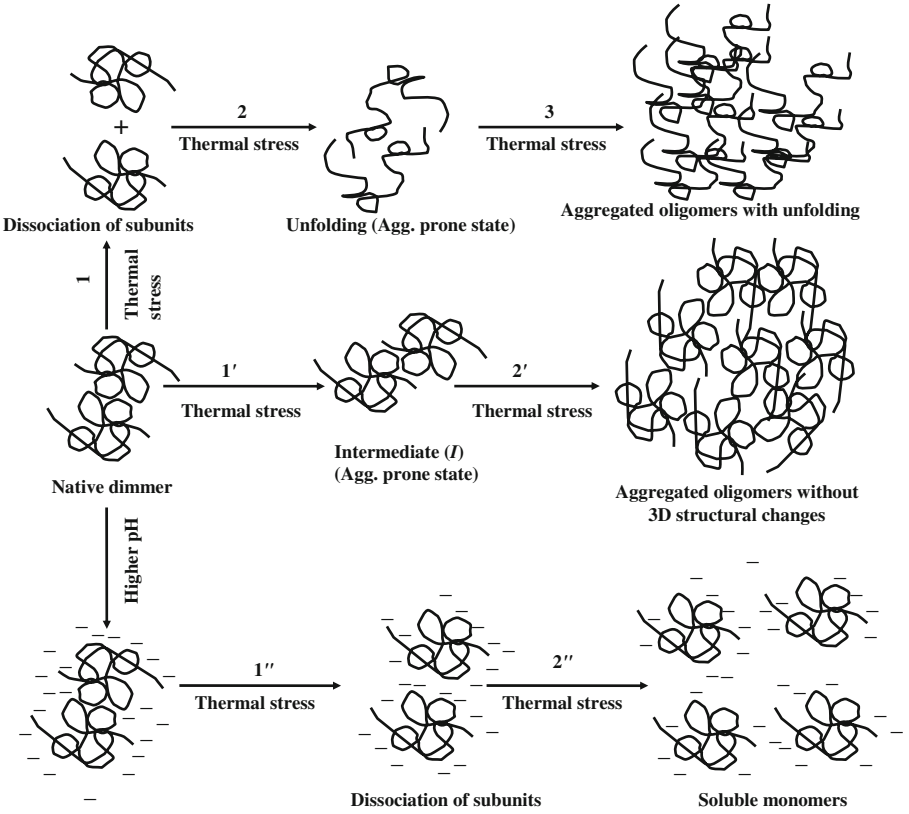

Scheme 1 A proposed schematic model for polymerization mechanism of HLADH aggregation pathway with two subunits as a dimer protein (similar model is possible for tetrameric YADH with four subunits)

for negative net charge effect on the aggregation suppression was proposed in reactions **1″** and **2″**. When the net charge of protein is high, the approach and interaction between distinct protein molecules is hindered by an overall effect of electrostatic repulsion. A decrease in the net charge leads to reduction in the extent of such repulsions, contributing to an acceleration of the aggregation process. At pH 8.5, HLADH and YADH have approximately −7 and −12 net charges, respectively. Therefore, each molecule carries a significant amount of negative charge to repel the other one. Our results demonstrate that the negative charges (−7 and −12) enforce sufficient strain and repulsion against other favorable forces of aggregation, namely hydrophobic interactions, preventing the aggregation at pH 8.5. Increasing pH>8.5 results in increased negative net charge and strain against close proximity and aggregation of ADHs.

It has been previously shown that heat-induced RNase A aggregation depends on the pH of solution [43]. Long incubation period of RNase at harsh conditions (75°C and pH 3.0), having a +16 net charge, led to the prevention of aggregation. While at higher pH with low net charge, RNase was easily aggregated. Thus, electrostatic repulsion was proposed to be responsible for the absence of aggregates at low pH [44]. Studying two homologous proteins AcP and HypF-N, able to form amyloid fibrils, showed higher hydrophobicity and a lower net charge contribution to the aggregation and amyloid formation. At the considered pH values, HypF-N, and AcP had a net charge of +1 and +5, respectively. HypF-N aggregated with a

rate constant 1,000 times faster than AcP [20]. In agreement with these findings and Scheme 1, the aggregation of both HLADH and YADH correlated inversely with the net charge at various pHs. In contrast, the two proteins differ considerably in their net charge values at lower pH. However, increasing the pH>8.5 results in compensation of this effect. In addition, comparison of these two enzymes implies minimum precipitation for YADH under heat stress because of higher negative net charge.

The pH is one of the important physical parameters for enzyme function either in vivo or in vitro and determines the unique conformation for enzyme's activity. This notion is consistent with our structural studies, discussed above. The higher net charge not only prevents aggregation but also has a favorable effect on enzyme function. The ability of pH to prevent ADH aggregation was considered as a result of net charge at the studied pH. These evidences suggest that charge–charge repulsion is effective in preventing ADH aggregation via the inhibition of building nucleus by *I* conformers.

Conclusion

The failure of correct folding of proteins leads to aggregation with severe functional deficit for biotechnological over-production of enzymes in vivo. A fundamental understanding of molecular processes, leading to misfolding and self-assembly of proteins, is involved in various diseases or biotechnological applications of enzyme, which can provide important information to help identify the appropriate routes to control these processes. Here, we have shown that charge–charge repulsion is effective in preventing the ADH aggregation under heat stress. We proposed a model for oligomeric ADHs aggregation and possibly other oligomeric enzymes in order to elucidate the correctness of the popular mechanism (**1**, **2**, and **3**), and the time-course of protein aggregation following 3D conformational changes. The net charge effect on preventing the appearance of an intermediate (*I*) molecule to build up nucleus defines that the attributes of electrostatic charged amino acids by site-directed mutagenesis may be important. In this way, effective substitutions of hydrophobic amino acid residues with the charged ones may be beneficial in preventing the protein aggregation at neutral pH.

Acknowledgements The financial supports of Research Institute for Fundamental Sciences (RIFS), University of Tabriz; Research Council of the University of Tehran; Iran National Science Foundation are gratefully acknowledged.

References

1. Burdette, D. S., Tchernajencko, V., & Zeikus, J. G. (2000). *Enzyme and Microbial Technology, 27*, 11–18. doi:10.1016/S0141-0229(00)00192-7.
2. Jörnvall, H., Persson, B., & Jeffery, J. (1987). *European Journal of Biochemistry, 167*, 195–201. doi:10.1111/j.1432-1033.1987.tb13323.x.
3. Niefind, K., Müller, J., Riebel, B., Hummel, W., & Schomburg, D. (2003). *Journal of Molecular Biology, 327*, 317–328. doi:10.1016/S0022-2836(03)00081-0.
4. Adolph, H. W., Zwart, P., Meijers, R., Hubatsch, I., Kiefer, M., Lamzin, V., et al. (2000). *Biochemistry, 39*, 12885–12897. doi:10.1021/bi001376s.
5. Saliola, M., Shuster, M., Jr., & Falcone, C. (1990). *Yeast (Chichester, England), 6*, 193–204. doi:10.1002/yea.320060304.

6. Williamson, V. M., & Paquin, C. E. (1987). *Molecular & General Genetics, 209*, 374–381. doi:10.1007/BF00329668.
7. Reid, M. F., & Fewson, C. A. (1994). *Critical Reviews in Microbiology, 20*, 13–56. doi:10.3109/10408419409113545.
8. Lortie, R., Fassouane, A., Laval, J. M., & Bourdillon, C. (1992). *Biotechnology and Bioengineering, 39*, 157–163. doi:10.1002/bit.260390206.
9. Whitesides, G. M., & Wong, C. H. (1985). *Angewandte Chemie & Angewandte Chemie International Edition in English, 24*, 617–638. doi:10.1002/anie.198506173.
10. Simon, H., Bader, J., Gunther, H., Neumann, S., & Thanos, J. (1985). *Angewandte Chemie International Edition in English, 24*, 539–553. doi:10.1002/anie.198505391.
11. Irwin, J. B., Lok, K. P., Huang, K. W. C., & Jones, J. B. (1978). *Journal of the Chemical Society Perkin. I, 12*, 1636–1641.
12. Hummel, W., & Kukla, M. R. (1989). *European Journal of Biochemistry, 184*, 1–13. doi:10.1111/j.1432-1033.1989.tb14983.x.
13. Danielsson, O., & Jcrnvall, H. (1992). *Proceedings of the National Academy of Sciences of the United States of America, 89*, 9247–9251. doi:10.1073/pnas.89.19.9247.
14. Bolivar, J. M., Wilson, L., Ferrarotti, S. A., Guisan, J. M., Fernandez-Lafuente, R., & Mateo, C. (2006). *Journal of Biotechnology, 125*, 85–94. doi:10.1016/j.jbiotec.2006.01.028.
15. Horwitz, J. (1992). *Proceedings of the National Academy of Sciences of the United States of America, 89*, 10449–10453. doi:10.1073/pnas.89.21.10449.
16. Guha, S., Manna, T. K., Das, K. P., & Bhattacharyya, B. (1998). *Journal of Biological Chemistry, 273*, 30077–30080. doi:10.1074/jbc.273.46.30077.
17. Clark, J., & Huang, Q. L. (1996). *National Academy Science USA, 93*, 15185–15189. doi:10.1073/pnas.93.26.15185.
18. Miroliaei, M., & Nemat-Gorgani, M. (2002). *The International Journal of Biochemistry & Cell Biology, 34*, 169–175. doi:10.1016/S1357-2725(01)00109-1.
19. Barzegar, A., Yousefi, R., Sharifzadeh, A., Dalgalarrondo, M., Chobert, J. M., Ganjali, M. R., et al. (2008). *International Journal of Biological Macromolecules, 42*, 392–399. doi:10.1016/j.ijbiomac.2008.01.008.
20. Calamai, M., Taddei, N., Stefani, M., Ramponi, G., & Chiti, F. (2003). *Biochemistry, 42*, 15078–15083. doi:10.1021/bi030135s.
21. Hashemnia, S., Moosavi-Movahedi, A. A., Ghourchian, H., Ahmad, F., Hakimelahi, G. H., & Saboury, A. A. (2006). *International Journal of Biological Macromolecules, 40*, 47–53. doi:10.1016/j.ijbiomac.2006.05.011.
22. Manning, M. C., Matsuura, J. E., Kendrick, B. S., Meyer, J. D., Dormish, J. J., Vrkljan, M., et al. (1995). *Biotechnology and Bioengineering, 48*, 506–512. doi:10.1002/bit.260480513.
23. Barzegar, A., Moosavi-Movahedi, A. A., Mahnam, K., Bahrami, H., & Sheibani, N. (2008). *Journal of Peptide Science, 14*, 1173–1182. doi:10.1002/psc.1055.
24. Pace, C. N., Alston, R. W., & Shaw, K. L. (2000). *Protein Science, 9*, 1395–1398. doi:10.1110/ps.9.7.1395.
25. Hoppe, W., Lohmann, W., & Markl, H. (1982). *& Ziegler, H*. Springer, New York: Biophysics.
26. Cantor, C. R., Schimmel, P. R., & Part, W. H., II. (1980). *Biophysical Chemistry*. NewYork: Freeman.
27. Barzegar, A., Moosavi-Movahedi, A. A., Rezaei-Zarchi, S., Saboury, A. A., Ganjali, M. R., Norouzi, P., et al. (2008). *Biotechnology and Applied Biochemistry, 49*, 203–211. doi:10.1042/BA20070031.
28. Camerini-Otero, R. D., & Day, L. A. (1978). *Biopolymers, 17*, 2241–2249. doi:10.1002/bip.1978.360170916.
29. Sund, H., & Theorell, H. (1963). Alcohol Dehydrogenases. In P. Boyer, H. Lardy & K. Myrback (Eds.), *The Enzymes (25 pp)* (2nd ed., Vol. VII). New York: Academic.
30. Ehrenberg, A., & Dalziel, K. (1958). *Acta Chemica Scandinavica, 12*, 465–469. doi:10.3891/acta.chem.scand.12-0465.
31. Li, H., Robertson, A. D., & Jensen, J. H. (2005). *Proteins, 61*, 704–721. doi:10.1002/prot.20660.
32. Srisailam, S., Kumar, T. K. S., Srimathi, T., & Yu, C. (2002). *Journal of the American Chemical Society, 124*, 1884–1888. doi:10.1021/ja012070r.
33. Yang, F., Lim, G. P., Begum, A. N., Ubeda, O. J., Simmons, M. R., Ambegaokar, S. S., et al. (2005). *Journal of Biological Chemistry, 280*, 5892–5901. doi:10.1074/jbc.M404751200.
34. Stigter, D., & Dill, K. A. (1990). *Biochemistry, 29*, 1262–1271. doi:10.1021/bi00457a023.
35. Otzen, D. E., Knudsen, B. R., Aachmann, F., Larsen, K. L., & Wimmer, R. (2002). *Protein Science, 11*, 1779–1787. doi:10.1110/ps.0202702.
36. Amani, M., Moosavi-Movahedi, A. A., Floris, G., Longu, S., Mura, A., Moosavi-Nejad, S. Z., et al. (2005). *The Protein Journal, 24*, 7842–7845. doi:10.1007/s10930-005-7842-5.
37. Poltorak, O. M., Chukhray, E. S., & Torshin, I. Y. (1998). *Biochemistry. Biokhimiia, 63*, 303–311.

38. Poltorak, O. M., Chukhray, E. S., Torshin, I. Y., Atyaksheva, L. F., Trevan, M. D., & Chaplin, M. F. (1999). *Journal of Molecular Catalysis. B, Enzymatic, 7*, 165–172.
39. Poltorak, O. M., Chukhray, E. S., Kozlenkov, A. A., Chaplin, M. F., & Trevan, M. D. (1999). *Journal of Molecular Catalysis. B, Enzymatic, 7*, 157–163.
40. Hassanisadi, M., Barzegar, A., Yousefi, R., Dalgalarrondo, M., Chobert, J. M., Haertle, T., et al. (2008). *Analytica Chimica Acta, 613*, 40–47. doi:10.1016/j.aca.2008.02.036.
41. Speed, M. A., King, J., & Wang, D. I. C. (1997). *Biotechnology and Bioengineering, 54*, 333–343. doi:10.1002/(SICI)1097-0290(19970520)54:4<333::AID-BIT6>3.0.CO;2-L.
42. Brown, P. H., & Schuck, P. (2006). *Biophysical Journal, 90*, 4651–4661. doi:10.1529/biophysj.106.081372.
43. Tsai, A. M., Van Zanten, J. H., & Betenbaugh, M. J. (1998). *Biotechnology and Bioengineering, 59*, 273–280. doi:10.1002/(SICI)1097-0290(19980805)59:3<273::AID-BIT2>3.0.CO;2-8.
44. Tsai, A. M., Van Zanten, J. H., & Betenbaugh, M. J. (1998). *Biotechnology and Bioengineering, 59*, 281–285. doi:10.1002/(SICI)1097-0290(19980805)59:3<281::AID-BIT3>3.0.CO;2-7.